Journal of Sound and Vibration (2002) **258**(4), 595–618
doi:10.1006/jsvi.2002.5090, available online at http://www.idealibrary.com on IDEAL®

ANALYTICAL AND NUMERICAL STUDY ON SPATIAL FREE VIBRATION OF NON-SYMMETRIC THIN-WALLED CURVED BEAMS

M.-Y. KIM AND N.-I. KIM

Department of Civil and Environmental Engineering, Sungkyunkwan University, 300 Chunchun, Jangan, Suwon, Kyunggi 440-746*, South Korea. E-mail: kmye@yurim.skku.ac.kr*

AND

B.-C. MIN

Pheonghwa Engineering, Seoul, South Korea

(*Received* 18 *June* 2001, *and in final form* 22 *February* 2002)

For spatial free vibration of non-symmetric thin-walled circular curved beams, an accurate displacement field is introduced by defining all displacement parameters at the centroidal axis and three total potential energy functionals are consistently derived by degenerating the potential energy for the elastic continuum to that for thin-walled curved beams. The closed-form solutions are newly obtained for in-plane and out-of-plane free vibration analysis of monosymmetric curved beams respectively. Also, two thin-walled curved beam elements are developed using the third and fifth order Hermitian polynomials. In order to illustrate the accuracy and the practical usefulness of the present method, analytical and numerical solutions by this study are presented and compared with previously published results or solutions by ABAQUS' the shell element. Particularly, effects of the thickness curvature as well as the inextensional condition are investigated on free vibration of curved beams with monosymmetric and non-symmetric cross-sections.

1. INTRODUCTION

Structural members having thin-walled curved open cross-sections, such as W section channel and angle, offer a high performance with minimum weight. Also, the construction cost of curved alignments associated with the substructuring has been found to be significantly reduced by the advent of the curved girder system. The accurate prediction of the natural frequencies corresponding to a vibration mode is of fundamental importance in the design of the thin-walled structure. And considerable research on the free vibration of curved beam element and curved girder bridge has been performed including effects of various parameters such as various boundary conditions, the initial stress, shear deformation, rotary inertia, extension of the neutral axis, elastic foundation, and variable curvatures and cross-sections.

Raveendranath *et al.* [1] investigated the performance of a curved beam finite element with coupled polynomial distribution for normal displacement and tangential displacement for in-plane flexural vibration of arches and Oh *et al.* [2] derived the governing equations of the free vibrations of non-circular arches based on the Timoshenko beam theory. Also it may be pointed out that intensive research [1–19] have been done on the

0022-460X/02/$35.00

in-plane free vibration of curved beams and particularly several authors [3–13] have investigated phenomena of transition of in-plane modes from extensional into inextensional that occur at certain combination of curvature and length of the beam. Other researchers have studied on the out-of-plane free vibrations [20–27] or both in-plane and out-of-plane free vibrations [28, 29] for curved beams. However, most of these researches are confined to in-plane and out-of-plane vibration of thin-walled curved beams with only symmetric cross-sections.

On the other hand, Gendy and Saleeb [30] developed a simple finite element model for the free vibration analysis of spatial behavior of curved beams with *arbitrary* cross-section considering the shear deformation and rotary inertia, but their study did not take into account effects of the thickness–curvature and the inextensional constraint on the spatial free vibration of curved beams. Also, Kim *et al*. [31, 32] presented a general theory for spatial stability of *non-symmetric* thin-walled curved beams.

In this paper, based on the study of Kim *et al*., an improved energy formulation for spatially coupled free vibration of non-symmetric thin-walled curved beams are consistently presented by introducing Vlasov's assumption and degenerating the total potential energy for the elastic continuum to that for the curved beam. In order to illustrate the accuracy and practical usefulness of this formulation, the analytical and numerical solutions evaluated by this study are presented and compared with previously published results or those by ABAQUS' shell element [33]. The important points presented are summarized as follows:

1. An accurate displacement field for the non-symmetric thin-walled cross-section is introduced by defining all displacement parameters at the centroid axis and taking into account the constant curvature.
2. Three potential energy functionals are consistently derived depending on whether the thickness–curvature effect and the inextensional condition of the centroidal axis are included or not.
3. The closed-form solutions are newly derived for in-plane and out-of-plane free vibration analysis of monosymmetric curved beams, respectively.
4. Two thin-walled curved beam elements corresponding to extensional and inextensional conditions are developed using the third and fifth order Hermitian polynomials.
5. The influences of the thickness–curvature effect and the inextensional condition on free vibration behaviors of curved beams with various end supports are investigated using the analytical and numerical method presented in the study.

2. PRINCIPLE OF VIRTUAL WORK

The global co-ordinates of the non-symmetric thin-walled curved beam are shown in Figure 1. In this paper, the following assumptions are adopted:

1. The thin-walled curved beam is linearly elastic and prismatic.
2. The cross-section is rigid with respect to in-plane deformation except for warping deformation.
3. The effects of shear deformations are negligible.

For free vibration analysis of the general continuum, the principle of virtual work is expressed as follows:

$$\int_V \tau_{ij}\delta e_{ij}\,\mathrm{d}V - \omega^2 \int_V \rho U_i \delta U_i\,\mathrm{d}V = \int_S T_i \delta U_i\,\mathrm{d}S, \tag{1}$$

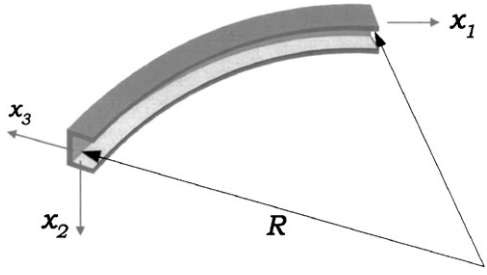

Figure 1. Co-ordinated system of non-symmetric thin-walled curved beam.

where τ_{ij} and e_{ij} are the stress and linear strain, respectively; ρ the density; ω the circular frequency; T_i the surface force, U_i the displacement; and δ denotes "virtual".

2.1. DISPLACEMENT FIELD OF THIN-WALLED CROSS-SECTION

Displacement parameters for the non-symmetric thin-walled cross-section defined at the cylindrical co-ordinate system (x_1, x_2, x_3) are shown in Figure 2. the x_1-axis coincides with the centroidal axis but x_2, x_3 are not necessarily principal inertia axes, e_2, e_3 are components of the position vector of the shear center in the local co-ordinate. U_x, U_y, U_z and ω_1, ω_2, ω_3 are rigid body translations and rotations of the cross-section about x_1, x_2, and x_3 axes, respectively. f is a warping parameter denoting the gradient of the twisting angle $\theta(=\omega_1)$. Under the assumption of the negligible shear deformation, rotational parameters ω_1, ω_3, f and an axial parameter g can be related with respect to rigid body translations and a twisting angle by Frenet's formula [34] as follows:

$$\omega_2 = -U_z' + \frac{U_x}{R}, \quad \omega_3 = U_y', \tag{2a, b}$$

$$f = -\theta' - \frac{U_y'}{R}, \quad g = U_x' + \frac{U_z}{R}, \tag{2c, d}$$

where the superscript 'prime' denotes the derivative with respect to x_1.

The displacement vector components of the arbitrary point on the thin-walled cross – section can be written as follows:

$$U_1 = U_x - x_2 U_y' - x_3\left(U_z' - \frac{U_x}{R}\right) - \left(\theta' + \frac{U_y'}{R}\right)\phi(x_2, x_3), \tag{3a}$$

$$U_2 = U_y - x_3\theta, \quad U_3 = U_z + x_2\theta, \tag{3b, c}$$

where ϕ is the normalized warping function defined at the centroid. Defining ϕ_s as the warping function at the shear center and considering the general thin-walled beam theory, a following relationship between ϕ and ϕ_s is obtained:

$$\phi = \phi_s + e_2 x_3 - e_3 x_2. \tag{4}$$

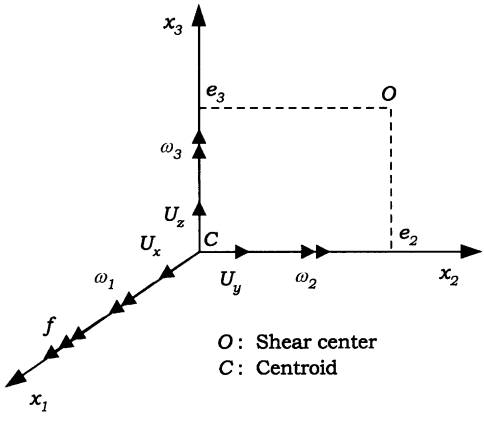

Figure 2. Notation for displacement parameters.

section properties used in this study are defined as follows:

$$
\begin{aligned}
I_2 &= \int_A x_3^2 \,\mathrm{d}A, \qquad I_3 = \int_A x_2^2 \,\mathrm{d}A, \qquad I_{23} = \int_A x_2 x_3 \,\mathrm{d}A,\\
I_\phi &= \int_A \phi^2 \,\mathrm{d}A, \qquad I_{\phi 2} = \int_A \phi x_3 \,\mathrm{d}A, \qquad I_{\phi 3} = \int_A \phi x_2 \,\mathrm{d}A,\\
I_{222} &= \int_A x_3^3 \,\mathrm{d}A, \qquad I_{223} = \int_A x_2 x_3^2 \,\mathrm{d}A, \qquad I_{233} = \int_A x_2^2 x_3 \,\mathrm{d}A,\\
I_{333} &= \int_A x_2^3 \,\mathrm{d}A, \qquad I_{\phi 22} = \int_A \phi x_3^2 \,\mathrm{d}A, \qquad I_{\phi 33} = \int_A \phi x_2^2 \,\mathrm{d}A,\\
I_{\phi 23} &= \int_A \phi x_3 x_2 \,\mathrm{d}A, \qquad I_{\phi\phi 2} = \int_A \phi^2 x_3 \,\mathrm{d}A, \qquad I_{\phi\phi 3} = \int_A \phi^2 x_2 \,\mathrm{d}A,
\end{aligned} \tag{5}
$$

where A, I_2, I_3, I_{23} and I_ϕ are the cross-sectional area, the second moment of inertia about x_2 and x_3 axes, product moment of inertia and the warping moment of inertia respectively. $I_{2\phi}(= I_2 e_2)$ and $I_{3\phi}(= -I_3 e_3)$ the product moments of inertia due to the normalized warping. $I_{ijk}(i,j,k = \phi, 2, 3)$ the third moments of inertia. The transformation equations between section properties defined at the centroid–centroid axis and those at the centroid–shear center axis may be referred to Reference [35].

2.2. STRAIN–DISPLACEMENT RELATIONS

The in-plane strains (e_{22}, e_{33}, e_{23}) are negligible according to the assumption of rigid deformation with respect to the in-plane. For the thin-walled curved beam, a complete set of linear strain–displacement relations is expressed as follows:

$$
\begin{aligned}
e_{11} &= \left(U_{1,1} + \frac{U_3}{R}\right)\frac{R}{R + x_3}\\
&= \left[U_x' + \frac{U_z}{R} - x_2\left(U_y'' - \frac{\theta}{R}\right) - x_3\left(U_z'' - \frac{U_x'}{R}\right) - \phi\left(\theta'' + \frac{U_y''}{R}\right)\right]\frac{R}{R + x_3},
\end{aligned} \tag{6a}
$$

$$
2e_{12} = U_{2,1}\frac{R}{R + x_3} + U_{1,2} = -x_3\left(\theta' + \frac{U_y'}{R}\right)\frac{R}{R + x_3} - \left(\theta' + \frac{U_y'}{R}\right)\phi_{,2}, \tag{6b}
$$

$$2e_{13} = \left(U_{3,1} - \frac{U_1}{R}\right)\frac{R}{R+x_3} + U_{1,3} = \left(x_2 + \frac{\phi}{R}\right)\left(\theta' + \frac{U_y'}{R}\right)\frac{R}{R+x_3} - \left(\theta' + \frac{U_y'}{R}\right)\phi_{,3}. \tag{6c}$$

2.3. TOTAL POTENTIAL ENERGY OF NON-SYMMETRIC THIN WALLED CURVED BEAMS

For the free vibration analysis of thin-walled curved beams vibrating harmonically, the total potential energy Π is expressed by the summation of the elastic strain energy U and the kinetic energy T:

$$\Pi = U - T, \tag{7}$$

where

$$U = \frac{1}{2}\int_L \int_A [Ee_{11}^2 + 4Ge_{12}^2 + 4Ge_{13}^2]\frac{R+x_3}{R}\,\mathrm{d}A\,\mathrm{d}x_1, \tag{8a}$$

$$T = \frac{1}{2}\rho\omega^2 \int_L \int_A [U_1^2 + U_2^2 + U_3^2]\frac{R+x_3}{R}\,\mathrm{d}A\,\mathrm{d}x_1, \tag{8b}$$

and E and G are Young's modulus and shear modulus respectively.

Now three types of the energy functional are derived in order to investigate the thickness-curvature effect as well as the inextensibility effect for the spatial free vibration of curved beams.

CASE 1: *Inclusion of both the extensibility and the thickness–curvature effects*. *CASE* 1 means a general energy formulation including both the extensibility condition and the thickness–curvature effect. In order to take into account the thickness–curvature effect consistently, the following approximation is adopted:

$$\frac{R}{R+x_3} \approx 1 - \frac{x_3}{R} + \frac{x_3^2}{R^2}. \tag{9}$$

Substituting the linear strain equation (6) into equation (8a), considering equation (9) and integrating over the cross-sectional area, the strain energy for the elastic continuum is degenerated to that for non-symmetric thin-walled beams as follows:

$$\begin{aligned} U^{case\ 1} = \frac{1}{2}\int_0^L \Bigg[& EA\left(U_x' + \frac{U_z}{R}\right)^2 + E\widehat{I_2}\left(U_z'' + \frac{U_z}{R^2}\right)^2 + E\widehat{I_3}\left(U_y'' - \frac{\theta}{R}\right)^2 \\ & + E\widehat{I_\phi}\left(\theta'' + \frac{U_y''}{R}\right)^2 + GJ\left(\theta' + \frac{U_y'}{R}\right)^2 + E\widehat{I_{\phi 2}}\left(U_z'' + \frac{U_z}{R^2}\right)\left(\theta'' + \frac{U_y''}{R}\right) \\ & + 2E\widehat{I_{\phi 3}}\left(U_y'' - \frac{\theta}{R}\right)\left(\theta'' + \frac{U_y''}{R}\right) + 2E\widehat{I_{23}}\left(U_y'' - \frac{\theta}{R}\right)\left(U_z'' + \frac{U_z}{R^2}\right)\Bigg]\,\mathrm{d}x_1, \end{aligned} \tag{10}$$

where

$$\begin{aligned} &\widehat{I_2} = I_2 - \frac{I_{222}}{R}, \qquad \widehat{I_3} = I_3 - \frac{I_{233}}{R}, \qquad \widehat{I_\phi} = I_\phi - \frac{I_{\phi\phi 2}}{R}, \\ &\widehat{I_{\phi 2}} = I_{\phi 2} - \frac{I_{\phi 22}}{R}, \qquad \widehat{I_{\phi 3}} = I_{\phi 3} - \frac{I_{\phi 23}}{R}, \qquad \widehat{I_{23}} = I_{23} - \frac{I_{223}}{R} \end{aligned} \tag{11}$$

and J is the St Venant torsion constant. Making use of the similar procedure, the kinetic energy T, relevant to the non-symmetric cross-section is obtained as follows:

$$\begin{aligned} T^{case\,1} = \frac{1}{2}\rho\omega^2 \int_0^L \Big[& A(U_x^2 + U_y^2 + U_z^2) + \widetilde{I}_0\theta^2 + \underline{\widetilde{I}_2\left(U_z' - \frac{U_x}{R}\right)^2} - 2\frac{I_2}{R}U_y\theta \\ & - 2\frac{I_2}{R}U_x\left(U_z' - \frac{U_x}{R}\right) + \underline{\tilde{I}_3 U_y'^2 + \widetilde{I}_\phi\left(\theta' + \frac{U_y'}{R}\right)^2} + 2\widetilde{I_{\phi 3}}U_y'\left(\theta' + \frac{U_y'}{R}\right) \\ & + 2\tilde{I}_{\phi 2}\left(U_z' - \frac{U_x}{R}\right)\left(\theta' + \frac{U_y'}{R}\right) - 2\frac{I_{\phi 2}}{R}U_x\left(\theta' + \frac{U_y'}{R}\right) \\ & + 2\frac{I_{223}}{R}U_y'\left(U_z' - \frac{U_x}{R}\right) + 2I_{23}\left(U_y'U_z' - \frac{2}{R}U_xU_y' + \frac{1}{R}U_z\theta\right)\Big]\,\mathrm{d}x_1, \end{aligned} \tag{12}$$

where

$$\begin{aligned} &\widetilde{I}_2 = I_2 + \frac{I_{222}}{R}, \qquad \widetilde{I}_3 = I_3 + \frac{I_{233}}{R}, \qquad \widetilde{I}_\phi = I_\phi + \frac{I_{\phi\phi 2}}{R}, \qquad \widetilde{I}_0 = I_2 + I_3, \\ &\widetilde{I_{\phi 2}} = I_{\phi 2} + \frac{I_{\phi 22}}{R}, \qquad \widetilde{I_{\phi 3}} = I_{\phi 3} + \frac{I_{\phi 23}}{R}, \qquad \widetilde{I}_0 = I_0 + \frac{I_{222} + I_{223}}{R} \end{aligned} \tag{13}$$

and the underlined terms in equations (12), (16), (19), and (21) denote rotary inertia effects.

CASE 2: *Inclusion of the thickness-curvature effect under the inextensibility condition*. A kinematic constraint is introduced in order to investigate the inextensibility effect on free vibration of curved beams as follows:

$$U_x' + \frac{U_z}{R} = 0. \tag{14}$$

Now, by using the inextensional condition (14), elimination of U_z in equations (10) and (12) leads to

$$\begin{aligned} U^{case\,2} = \frac{1}{2}\int_0^L \Bigg[& E\widehat{I}_2\left(RU_x''' + \frac{U_x'}{R}\right)^2 + E\widehat{I}_3\left(U_y'' - \frac{\theta}{R}\right)^2 + E\widehat{I}_\phi\left(\theta'' + \frac{U_y''}{R}\right)^2 \\ & + GJ\left(\theta' + \frac{U_y'}{R}\right)^2 - 2E\widehat{I_{\phi 2}}\left(RU_x''' + \frac{U_x'}{R}\right)\left(\theta'' + \frac{U_y''}{R}\right) \\ & + 2E\widehat{I_{\phi 3}}\left(U_y'' - \frac{\theta}{R}\right)\left(\theta'' + \frac{U_y''}{R}\right) - 2E\widehat{I_{23}}\left(U_y'' - \frac{\theta}{R}\right)\left(RU_x''' + \frac{U_x'}{R}\right)\Bigg]\,\mathrm{d}x_1, \end{aligned} \tag{15}$$

and

$$\begin{aligned} T^{case\,2} = \frac{1}{2}\rho\omega^2 \int_0^L \Big[& A(U_x^2 + U_y^2 + R^2U_x'^2) + \widetilde{I}_0\theta^2 + \underline{\widetilde{I}_2\left(RU_x'' + \frac{U_x}{R}\right)^2} - 2\frac{I_2}{R}U_y\theta \\ & + 2\frac{I_2}{R}U_x\left(RU_x'' + \frac{U_x}{R}\right) + \underline{\widetilde{I}_3 U_y'^2 + \widetilde{I}_\phi\left(\theta' + \frac{U_y'}{R}\right)^2} + 2\widetilde{I_{\phi 3}}U_y'\left(\theta' + \frac{U_y'}{R}\right) \\ & - 2\widetilde{I_{\phi 2}}\left(RU_x'' + \frac{U_x}{R}\right)\left(\theta' + \frac{U_y'}{R}\right) - 2\frac{I_{\phi 2}}{R}U_x\left(\theta' + \frac{U_y'}{R}\right) \\ & - 2\frac{I_{223}}{R}U_y'\left(RU_x'' + \frac{U_x}{R}\right) - 2I_{23}\left(RU_x''U_y' + \frac{2}{R}U_xU_y' + U_x'\theta\right)\Big]\,\mathrm{d}x_1 \end{aligned} \tag{16}$$

CASE 3: *Disregard of the thickness-curvature effect under the extensibility condition*. In case of disregarding the thickness–curvature effect but allowing the extensibility, the

following approximations are used in this study:

$$\frac{R}{R+x_3} \approx 1, \qquad \frac{R+x_3}{R} \approx 1. \tag{17a, b}$$

As a result, the integration of equations (8a) and (8b) over the cross-section under the condition (17) leads to equations (18) and (19) respectively.

$$\begin{aligned} U^{case\ 3} = \frac{1}{2}\int_0^L \Bigg[& EA\left(U_x' + \frac{U_z}{R}\right)^2 + EI_2\left(U_z'' - \frac{U_x'}{R^2}\right)^2 + EI_3\left(U_y'' - \frac{\theta}{R}\right)^2 \\ & + EI_\phi\left(\theta'' + \frac{U_y''}{R}\right)^2 + GJ\left(\theta' + \frac{U_y'}{R}\right)^2 + 2EI_{\phi 2}\left(U_z'' - \frac{U_x'}{R}\right)\left(\theta'' + \frac{U_y''}{R}\right) \\ & + 2EI_{\phi 3}\left(U_y'' - \frac{\theta}{R}\right)\left(\theta'' + \frac{U_y''}{R}\right) + 2EI_{23}\left(U_y'' - \frac{\theta}{R}\right)\left(U_z'' - \frac{U_x'}{R}\right)\Bigg]\,\mathrm{d}x_1, \end{aligned} \tag{18}$$

and

$$\begin{aligned} T^{case\ 3} = \frac{1}{2}\rho\omega^2\int_0^L \Bigg[& A(U_x^2 + U_y^2 + U_z^2) + I_0\theta^2 + \underline{I_2\left(U_z' - \frac{U_x}{R}\right)^2 + I_3 U_y'^2 + I_\phi\left(\theta' + \frac{U_y'}{R}\right)^2} \\ & + 2I_{\phi 3}U_y'\left(\theta' + \frac{U_y'}{R}\right) + 2I_{\phi 2}\left(U_z' - \frac{U_x}{R}\right)\left(\theta' + \frac{U_y'}{R}\right) + 2I_{23}U_y'\left(U_z' - \frac{U_x}{R}\right)\Bigg]\,\mathrm{d}x_1. \end{aligned} \tag{19}$$

Here it should be noted that shear deformation effects due to shear forces are neglected but all rotary inertia terms are included in deriving three energy functionals.

3. ANALYTICAL SOLUTION OF MONOSYMMETRIC THIN-WALLED CURVED BEAMS

For curved beams with the monosymmetric cross-section for x_3 axis (see Figure 1), the following section properties become zero:

$$I_{223} = I_{\phi 2} = I_{\phi 22} = I_{23} = 0 \tag{20}$$

so that in-plane and out-of-plane modes are decoupled. In this section, the closed-form solutions for monosymmetric curved beams are newly derived for in-plane behaviors under arbitrary boundary conditions and out-of-plane behaviors under the simply supported condition respectively.

3.1. IN-PLANE FREE VIBRATION

Retaining only the terms relevant to the in-plane deformation of monosymmetric thin-walled curved beams, three total potential energies derived in Section 2 is expressed as follows:

$$\begin{aligned} \Pi_{in}^{case\ 1} = \frac{1}{2}\int_0^L \Bigg[& EA\left(U_x' + \frac{U_z}{R}\right)^2 + E\widehat{I}_2\left(U_z'' + \frac{U_z}{R^2}\right)^2 - \rho\omega^2\Bigg\{A(U_x^2 + U_z^2) \\ & + \underline{\widetilde{I}_2\left(U_z' - \frac{U_x}{R}\right)^2} - 2\frac{I_2}{R}U_x\left(U_z' - \frac{U_x}{R}\right)\Bigg\}\Bigg]\,\mathrm{d}x_1, \end{aligned} \tag{21a}$$

$$\Pi_{in}^{case\ 2} = \frac{1}{2}\int_0^L \left[E\widehat{I}_2 \left(RU_x''' + \frac{U_x'}{R} \right)^2 - \rho\omega^2 \left\{ A(U_x^2 + R^2 U_x'^2) + \underline{\widetilde{I}_2 \left(RU_x'' + \frac{U_x}{R} \right)^2} + 2\frac{I_2}{R} U_x \left(RU_x'' + \frac{U_x}{R} \right) \right\} \right] \mathrm{d}x_1, \tag{21b}$$

$$\Pi_{in}^{case\ 3} = \frac{1}{2}\int_0^L \left[EA \left(U_x' + \frac{U_z}{R} \right)^2 + EI_2 \left(U_z'' - \frac{U_x'}{R^2} \right)^2 - \rho\omega^2 \left\{ A(U_x^2 + U_z^2) + \underline{I_2 \left(U_z' - \frac{U_x}{R} \right)^2} \right\} \right] \mathrm{d}x_1, \tag{21c}$$

On the other hand, in order to investigate the extensional and inextensional in-plane vibrational behaviors of curved beams with rectangular sections, Chidamparam and Leissa [8] considered two potential energies neglecting the rotary inertia effects as follows:

$$\Pi_{in}^{extenstion\ [8]} = \frac{1}{2}\int_0^L \left[EA \left(U_x' + \frac{U_z}{R} \right)^2 - EI_2 \left(U_z'' - \frac{U_x'}{R^2} \right)^2 - \rho\omega^2 A(U_x^2 + U_z^2) \right] \mathrm{d}x_1, \tag{22a}$$

$$\Pi_{in}^{inextenstion\ [8]} = \frac{1}{2}\int_0^L \left[EI_2 \left(RU_x''' + \frac{U_x'}{R} \right)^2 - \rho\omega^2 A(U_x^2 + R^2 U_x'^2) \right] \mathrm{d}x_1, \tag{22b}$$

Now, the derivation procedure of the closed-form solution is presented for in-plane vibration behaviors. The following simultaneous ordinary differential equations and boundary conditions are obtained by applying the varational principle to the potential energy (21a).

$$EAU_x'' + \rho\omega^2 \left(A + \frac{\widetilde{I}_2}{R^2} + 2\frac{I_2}{R^2} \right) U_x + \left(\frac{EA}{R} - \rho\omega^2 \frac{\widetilde{I}_2}{R} - \rho\omega^2 \frac{I_2}{R} \right) U_z' = 0, \tag{23a}$$

$$E\widehat{I}_2 U_z{}^{\mathrm{IV}} + \left(2\frac{E\widehat{I}_2}{R^2} + \rho\omega^2 \widetilde{I}_2 \right) U_z'' + \left(\frac{EA}{R^2} + \frac{E\widehat{I}_2}{R^4} - -\rho\omega^2 A \right) U_z + \left(\frac{EA}{R} - \rho\omega^2 \frac{\widetilde{I}_2}{R} - \rho\omega^2 \frac{I_2}{R} \right) U_x' = 0, \tag{23b}$$

and

$$\delta U_x = 0 \quad \text{or} \quad EA \left(U_x' + \frac{U_z}{R} \right) + \frac{E\widehat{I}_2}{R} \left(U_z'' + \frac{U_z}{R^2} \right) = 0 \quad \text{at } x_1 = 0, L, \tag{24a}$$

$$\delta U_z = 0 \quad \text{or} \quad E\hat{I}_2 \left(U_z''' + \frac{U_z'}{R^2} \right) + \rho\omega^2 \widetilde{I}_2 \left(U_z' - \frac{U_x}{R} \right) - \rho\omega^2 I_2 \frac{U_x}{R} = 0 \quad \text{at } x_1 = 0, L, \tag{24b}$$

$$\delta \left(-U_z' + \frac{U_x}{R} \right) = 0 \quad \text{or} \quad -E\hat{I}_2 \left(U_z'' + \frac{U_z}{R^2} \right) = 0 \quad \text{at } x_1 = 0, L, \tag{24c}$$

Elimination of U_z from equation (23) leads to the sixth order homogeneous differential equation as follows:

$$U_x{}^{\mathrm{VI}} + a_1 U_x{}^{\mathrm{IV}} + a_2 U_x'' + a_3 U_x = 0, \tag{25}$$

where

$$a_1 = \frac{1}{EA\widehat{I}_2}\left\{\rho\omega^2\widehat{I}_2\left(A + \frac{\widetilde{I}_2}{R^2} + 2\frac{I_2}{R^2}\right) + A\left(2\frac{E\widehat{I}_2}{R^2} + \rho\omega^2\widetilde{I}_2\right)\right\}, \tag{26a}$$

$$a_2 = \frac{1}{E^2A\widehat{I}_2}\left\{\rho\omega^2\widehat{I}_2\left(A + \frac{\widetilde{I}_2}{R^2} + 2\frac{I_2}{R^2}\right)\left(2\frac{E\widehat{I}_2}{R^2} + \rho\omega^2\widetilde{I}_2\right)\right.$$

$$\left. - \frac{\{EA - \rho\omega^2(\widetilde{I}_2 + I_2)\}^2}{R^2} + \frac{EA(EAR^2 + E\widehat{I}_2 - \rho\omega^2AR^4}{R^4}\right\}, \tag{26b}$$

$$a_3 = \frac{\rho\omega^2(EAR^2 + E\widehat{I}_2 - \rho\omega^2A)}{R^4E^2A\widehat{I}_2}\left(A + \frac{\widetilde{I}_2}{R^2} + 2\frac{I_2}{R^2}\right). \tag{26c}$$

The general solution of equation (25) may be assumed as

$$U_x = \sum_{i=1}^{6} b_i e^{\psi_i x_1}, \tag{27}$$

where ψ_i are the roots of the characteristic equation (28).

$$\psi^6 + a_1\psi^4 + a_2\psi^2 + a_3 = 0. \tag{28}$$

In order to determine the root of above equation, let $\psi^2 = S$. Then equation (28) becomes the cubic equation with respect to S which can be solved using the standard procedure [25]. In addition, the mathematical expression for U_z can be easily obtained by substituting equation (27) into equation (23) and integrating equation (23).

On the other hand, the six conditions corresponding to a specific boundary condition can be determined using equation (24) consisting of the geometric and essential boundary conditions. For example, in case of the simply supported condition, the boundary condition is as follows:

$$U_x = U_z = U_z'' = 0 \quad \text{at } x_1 = 0, L. \tag{29}$$

Now by applying the six boundary conditions to expressions for U_x and U_z, the following homogeneous equations are obtained:

$$\mathbf{K}(\boldsymbol{\omega})\mathbf{c} = \mathbf{0} \quad \text{where } \mathbf{c} = \langle c_1, c_2, c_3, c_4, c_5, c_6\rangle^{\mathrm{T}}. \tag{30a, b}$$

Finally, natural frequencies of thin-walled curved beams can be determined form the condition that the determinant of the matrix $\mathbf{K}$ is zero.

$$\det|\mathbf{K}(\boldsymbol{\omega})| = 0. \tag{31}$$

Also, natural frequencies of in-plane free vibration corresponding to *CASE* 2 and *CASE* 3 can be determined through the similar procedures.

3.2. OUT -OF-PLANE FREE VIBRATION

Now the out-of-plane free vibration problem of simply supported thin-walled curved beams with monosymmetric sections is considered. By retaining terms only relevant to the lateral displacement U_y and the torsional rotation θ in equations (10) and (12), the total potential energy of *CASE* 1 corresponding to out-of-plane vibration modes is obtained

as follows:

$$\Pi_{out}^{case\ 1} = \frac{1}{2}\int_0^L \left[E\widehat{I_3}\left(U_y'' - \frac{\theta}{R}\right)^2 + GJ\left(\theta' + \frac{U_y'}{R}\right)^2 + E\widehat{I_\phi}\left(\theta'' + \frac{U_y''}{R}\right)^2 + 2E\widehat{I_{\phi 3}}\left(U_y'' - \frac{\theta}{R}\right)\left(\theta'' + \frac{U_y''}{R}\right) - \rho\omega^2\left\{ A U_y^2 + \widetilde{I_0}\theta^2 + \widetilde{I_3} U_y'^2 . + \widetilde{I_\phi}\left(\theta' + \frac{U_y'}{R}\right)^2 - 2\frac{I_2}{R} U_y\theta + 2\widetilde{I_{\phi 3}} U_y'\left(\theta' + \frac{U_y'}{R}\right)\right\}\right] \mathrm{d}x_1 \tag{32a}$$

and for *CASE* 3

$$\Pi_{out}^{case\ 3} = \frac{1}{2}\int_0^L \left[EI_3\left(U_y'' - \frac{\theta}{R}\right)^2 + GJ\left(\theta' + \frac{U_y'}{R}\right)^2 + EI_\phi\left(\theta'' + \frac{U_y''}{R}\right)^2 + 2EI_{\phi 3}\left(U_y'' - \frac{\theta}{R}\right)\left(\theta'' + \frac{U_y''}{R}\right) - \rho\omega^2\left\{ A U_y^2 + \widetilde{I_0}\theta^2 + I_3 U_y'^2 . + I_\phi\left(\theta' + \frac{U_y'}{R}\right)^2 + 2I_{\phi 3} U_y'\left(\theta' + \frac{U_y'}{R}\right)\right\}\right] \mathrm{d}x_1 . \tag{32b}$$

Then for out-of-plane vibration behavior under simply supported conditions, governing equations and boundary conditions of *CASE* 1 are obtained as equations (33) and (34) respectively.

$$E\widehat{I_3}\left(U_y^{\mathrm{IV}} - \frac{\theta''}{R}\right) - GJ\left(\frac{U_y''}{R^2} + \frac{\theta''}{R}\right) + E\widehat{I_\phi}\left(\frac{U_y^{\mathrm{IV}}}{R^2} + \frac{\theta^{\mathrm{IV}}}{R}\right) + E\widehat{I_{\phi 3}}\left(\frac{2}{R} U_y^{\mathrm{IV}} + \theta^{\mathrm{IV}} - \frac{\theta''}{R^2}\right) - \rho\omega^2\left\{ A U_y - \widetilde{I_3} U_y'' - \widetilde{I_\phi}\left(\frac{U_y''}{R^2} + \frac{\theta''}{R}\right) - \frac{I_2}{R}\theta - \widetilde{I_{\phi 3}}\left(\frac{2}{R} U_y'' + \theta''\right)\right\} = 0, \tag{33a}$$

$$E\widehat{I_3}\left(\frac{\theta}{R^2} - \frac{U_y''}{R}\right) - GJ\left(\frac{U_y''}{R} + \theta''\right) + E\widehat{I_\phi}\left(\frac{U_y^{\mathrm{IV}}}{R} + \theta^{\mathrm{IV}}\right) + E\widehat{I_{\phi 3}}\left(U_y^{\mathrm{IV}} - \frac{U_y''}{R^2} - \frac{2}{R}\theta''\right) - \rho\omega^2\left\{ \widetilde{I_0}\theta - \widetilde{I_\phi}\left(\frac{U_y''}{R} + \theta''\right) - \frac{I_2}{R} U_y - \widetilde{I_{\phi 3}} U_y''\right\} = 0. \tag{33b}$$

and

$$\delta U_y = 0, \quad \delta\theta = 0 \quad \text{at } x_1 = 0, L, \tag{34a, b}$$

$$M_3 = E\widehat{I_3}\left(U_y'' - \frac{\theta}{R}\right) + E\widehat{I_{\phi 3}}\left(\frac{U_y''}{R} + \theta''\right) = 0 \quad \text{at } x_1 = 0, L, \tag{34c}$$

$$M_\phi = E\widehat{I_\phi}\left(\frac{U_y''}{R} + \theta''\right) + E\widehat{I_{\phi 3}}\left(U_y'' - \frac{\theta}{R}\right) = 0 \quad \text{at } x_1 = 0, L. \tag{34d}$$

The lateral displacement U_y and the torsional rotation θ for lateral motion of simply supported curved beams may be assumed as follows:

$$U_y = B\sin(\lambda x_1), \quad \theta = D\sin(\lambda x_1), \tag{35}$$

where $\lambda = n\pi/L$, $n = 1, 2, 3, \ldots$. It should be noticed that the above functions exactly satisfy the geometric and *essential* boundary conditions as well as governing equations because all equations contain only even derivative terms of U_y and θ with respect to x_1.

In the above equation, B and D are unknown coefficients (amplitude) and λ indicates the vibration mode of the curved beam. After substituting displacement functions into equation (33), the following characteristic equation is obtained by invoking the stationarity of Π with respect to the unknown coefficients:

$$\begin{bmatrix} K_{11} & K_{12} \\ K_{21} & K_{22} \end{bmatrix} \begin{Bmatrix} B \\ D \end{Bmatrix} = \begin{Bmatrix} 0 \\ 0 \end{Bmatrix}, \tag{36}$$

where

$$K_{11} = E\widehat{I}_3\lambda^4 + GJ\frac{\lambda^2}{R^2} + E\widehat{I}_\phi\frac{\lambda^4}{R^2} + 2E\widehat{I_{\phi 3}}\frac{\lambda^4}{R} - \rho\omega^2\left(A + \widetilde{I}_3\lambda^2 + \widetilde{I}_\phi\frac{\lambda^2}{R^2} + 2\widetilde{I_{\phi 3}}\frac{\lambda^2}{R}\right), \tag{37a}$$

$$K_{12} = E\widehat{I}_3\frac{\lambda^2}{R} + GJ\frac{\lambda^2}{R} + E\widehat{I}_\phi\frac{\lambda^4}{R} + E\widehat{I_{\phi 3}}\left(\lambda^4 + \frac{\lambda^2}{R^2}\right) - \rho\omega^2\left(\widetilde{I}_\phi\frac{\lambda^2}{R} - \frac{I_2}{R} + \widetilde{I_{\phi 3}}\lambda^2\right), \tag{37b}$$

$$K_{21} = K_{12}, \tag{37c}$$

$$K_{22} = E\widehat{I}_3\frac{1}{R^2} + GJ\lambda^2 + E\widehat{I}_\phi\lambda^4 + 2E\widehat{I_{\phi 3}}\frac{\lambda^2}{R} - \rho\omega^2(\widetilde{I}_0 + \widetilde{I}_\phi\lambda^2). \tag{37d}$$

For non-trivial solution, a quadratic equation for ω^2 is obtained by equating the determinant of equation (36) to zero.

$$C_1\omega^4 + C_2\omega^2 + C_3 = 0, \tag{38}$$

where

$$\begin{aligned} C_1 = \rho^2[&R^2\widetilde{I}_3\widetilde{I}_\phi\lambda^4 + R^2\widetilde{I}_3\widetilde{I}_0\lambda^2 + R^2A\widetilde{I}_\phi\lambda^2 + 2I_2\widetilde{I}_\phi\lambda^2 + \widetilde{I}_0\widetilde{I}_\phi\lambda^2 \\ &+ 2RI_2\widetilde{I_{\phi 3}}\lambda^2 - R^2\widetilde{I_{\phi 3}}^2\lambda^4 + 2R\widetilde{I}_0\widetilde{I_{\phi 3}}\lambda^2 - I_2^2 + R^2A\widetilde{I}_0], \end{aligned} \tag{39a}$$

$$\begin{aligned} C_2 = -\frac{\rho}{R^2}[&R^4E\widehat{I}_\phi\widetilde{I}_3\lambda^6 - 2R^4E\widehat{I_{\phi 3}}\widetilde{I_{\phi 3}}\lambda^6 + R^4E\widehat{I}_3\widetilde{I}_\phi\lambda^6 + 2R^3I_2E\widehat{I_{\phi 3}}\lambda^4 \\ &+ R^4AE\widehat{I}_\phi\lambda^4 + 2R^2I_2E\widehat{I}_\phi\lambda^4 + R^4\widetilde{I}_3GJ\lambda^4 + 2R^3E\widehat{I}_3\widetilde{I_{\phi 3}}\lambda^4 \\ &+ R^4\widetilde{I}_0E\widehat{I}_3\lambda^4 + 2R^3\widetilde{I}_0E\widehat{I_{\phi 3}}\lambda^4 + R^2\widetilde{I}_0E\widehat{I}_\phi\lambda^4 + 2R^3E\widehat{I_{\phi 3}}\widetilde{I}_3\lambda^4 \\ &+ 2R^2E\widehat{I_{\phi 3}}\widetilde{I_{\phi 3}}\lambda^4 - 2R^2E\widehat{I}_3\widetilde{I}_\phi\lambda^4 + R^4AGJ\lambda^2 + 2R^2I_2GJ\lambda^2 \\ &+ 2R^2I_2E\widehat{I}_3\lambda^2 + 2R^3AE\widehat{I_{\phi 3}}\lambda^2 + 2RI_2E\widehat{I_{\phi 3}}\lambda^2 + R^2E\widehat{I}_3\widetilde{I}_3\lambda^2 \\ &+ R^2\widetilde{I}_0GJ\lambda^2 + 2RE\widehat{I}_3\widetilde{I_{\phi 3}}\lambda^2 + E\widehat{I}_3\widetilde{I}_\phi\lambda^2 + R^2AE\widehat{I}_3], \end{aligned} \tag{39b}$$

$$C_3 = \frac{E\lambda^2}{R^2}(R^2\lambda^2 - 1)^2(E\hat{I}_3\hat{I}_\phi\lambda^2 + GJ\hat{I}_3 - E\hat{I}_{\phi 3}^2\lambda^2). \tag{39c}$$

In case of *CASE* 3, natural frequencies for out-of-plane free vibration can be determined by applying the similar procedures to the energy functional (32b).

4. THIN-WALLED CURVED BEAM ELEMENT

For spatial free vibration analysis of curved beams, two types of non-symmetric thin-walled curved beam elements associated with the extensional and the inextensional theory, respectively, are introduced in this section.

4.1. THE CURVED BEAM ELEMENT ALLOWING THE EXTENSIBILITY

Figure 3 shows the nodal displacement vector of thin-walled curved beam element including restrained warping effect. In order to accurately express the deformation of element, pertinent shape functions are necessary. In this study, the third order Hermitian polynomials are adopted to interpolate displacement parameters that are defined at the centroid axis. This curved beam element has two nodes and eight degrees of freedom per a node. As a results, the element displacement parameters U_x, U_y, U_z, θ can be interpolated with respect to the nodal displacements as follows:

$$U_x = h_1 u^p + h_2 g^p + h_3 u^q + h_4 g^q, \quad U_y = h_1 v^p + h_2 \omega_3^p + h_3 v^q + h_4 \omega_3^q, \tag{40a, b}$$

$$U_z = h_1 w^p - h_2 \omega_2^p + h_3 w^q - h_4 w_2^q, \quad \theta = h_1 \omega_1^p - h_2 f^p + h_3 \omega_1^q - h_4 f^q, \tag{40c, d}$$

where

$$\begin{aligned} &u^p = U_x(0), \quad v^p = U_y(0), \quad w^p = U_z(0), \quad \omega_1^p = \theta(0), \\ &\omega_2^p = -U_z'(0), \quad \omega_3^p = U_y'(0), \quad f^p = -\theta'(0), \quad g^p = U_x'(0) \end{aligned} \tag{41}$$

and h_i is the third order Hermitian polynomials as follows:

$$\begin{aligned} &h_1 = 2\xi^3 - 3\xi^2 + 1, \quad h_2 = (\xi^3 - 2\xi^2 + \xi)L, \\ &h_3 = -2\xi^3 + 3\xi^2, \quad h_4 = (\xi^3 - \xi^2)L, \end{aligned} \tag{42}$$

where

$$\xi = x_1/L.$$

Substituting the interpolating functions, material and cross-sectional properties into equations (10) and (12) including the thickness–curvature effects and equations (18) and (19) neglecting them and integrating along the element length, the total potential energy of thin-walled curved beam element is obtained in matrix form as

$$\Pi = \frac{1}{2}\mathbf{U}_e^{\mathrm{T}}(\mathbf{K}_e - \omega^2 \mathbf{M}_e)\mathbf{U}_e, \tag{43}$$

where

$$\mathbf{U}_e = \langle u^p, v^p, w^p, \omega_1^p, \omega_2^p, \omega_3^p, f^p, g^p, u^q, v^q, w^q, \omega_1^q, \omega_2^q, \omega_3^q, f^q, g^q \rangle. \tag{44}$$

In the above equation, $\mathbf{K}_e$ and $\mathbf{M}_e = 16 \times 16$ element elastic stiffness and mass matrices in local co-ordinate, respectively; $\mathbf{U}_e$ the nodal displacement vector. Stiffness and mass matrices are evaluated using the Gauss integration scheme. Before assembling element matrices into global matrices, it is necessary to introduce the following rotational and axial nodal displacement components including curvature effect:

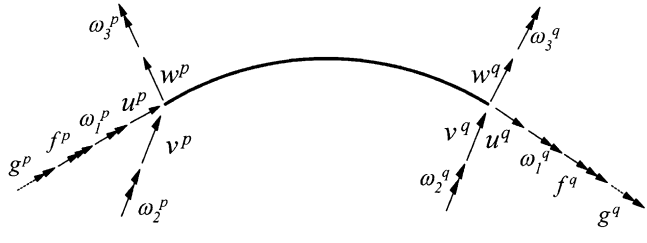

Figure 3. Nodal displacement vector of curved beam element with extensional theory.

$$\hat{\omega}_2^p = -U_z'(0) + \frac{U_x(0)}{R} = \hat{\omega}_2^p + \frac{u^p}{R}, \tag{45a}$$

$$\hat{f}^p = -\theta'(0) - \frac{U_y'(0)}{R} = f^p - \frac{\omega_3^p}{R}, \tag{45b}$$

$$\hat{g}^p = U_x'(0) + \frac{U_z(0)}{R} = g^p + \frac{w^p}{R}. \tag{45c}$$

For the evaluation of the element stiffness matrix corresponding to the newly defined nodal displacement components, the transformation equation between the nodal displacement vector $\mathbf{U}_e$ and the new displacement vector $\widehat{\mathbf{U}_e}$ consisting the effect of curvature is introduced as follows:

$$\mathbf{U}_a = \mathrm{T}_1 \hat{\mathbf{U}}_a, \quad a = p, q, \tag{46}$$

where

$$\mathbf{U}_a^{\mathrm{T}} = \{u^a\ v^a\ w^a\ \omega_1^a\ \omega_2^a\ \omega_3^a\ f^a\ g^a\}, \quad \widehat{\mathbf{U}_a^T} = \{u^a\ v^a\ w^a\ \omega_1^a\ \widehat{\omega_2^a}\ \omega_3^a\ \widehat{f^a}\ \widehat{g^a}\}. \tag{47}$$

and

$$T_1 = \left[\begin{array}{cccc|cccc} 1 & \cdot & \cdot & \cdot & \cdot & \cdot & \cdot & \cdot \\ \cdot & 1 & \cdot & \cdot & \cdot & \cdot & \cdot & \cdot \\ \cdot & \cdot & 1 & \cdot & \cdot & \cdot & \cdot & \cdot \\ \cdot & \cdot & \cdot & 1 & \cdot & \cdot & \cdot & \cdot \\ \hline -1/R & \cdot & \cdot & \cdot & 1 & \cdot & \cdot & \cdot \\ \cdot & \cdot & \cdot & \cdot & \cdot & 1 & \cdot & \cdot \\ \cdot & \cdot & \cdot & \cdot & \cdot & 1/R & 1 & \cdot \\ \cdot & \cdot & -1/R & \cdot & \cdot & \cdot & \cdot & 1 \end{array}\right]. \tag{48}$$

Transforming equation (43) using equation (48) and invoking the stationary condition, the eigenvalue problem is obtained as follows:

$$\widehat{\mathbf{K}_e}\widehat{\mathbf{U}_e}, \quad \omega^2 = \widehat{\mathbf{M}_e}\widehat{\mathbf{U}_e}, \tag{49}$$

where

$$\widehat{\mathbf{U}_e} = \langle u^p, v^p, w^p, \omega_1^p, \widehat{\omega_2^p}, \omega_3^p, \widehat{f^p}, \widehat{g^p}, u^q, v^q, w^q, \omega_1^q, \widehat{\omega_2^q}, \omega_3^q, \widehat{f^q}, \widehat{g^q} \rangle \tag{50}$$

and matrices and vectors in equation (49) are evaluated as follows:

$$\hat{\mathbf{K}}_e = \mathbf{T}^{\mathrm{T}} \mathbf{K}_e \mathbf{T}, \quad \mathbf{U}_e = \mathbf{T}\hat{\mathbf{U}}_e, \tag{51}$$

where

$$T = \left[\begin{array}{c:c} T_1 & \cdot \\ \hdashline \cdot & T_1 \end{array}\right]. \tag{52}$$

Now, using the direct stiffness method, the matrix equilibrium equation for the elastic free vibration analysis of non-symmetric thin-walled curved beam is obtained as follows:

$$\mathbf{K}_E \mathbf{U} = \omega^2 \mathbf{M}_E \mathbf{U} \tag{53}$$

where $\mathbf{K}_E$ and $\mathbf{M}_E$ are global elastic stiffness and mass matrices respectively.

4.2. THE CURVED BEAM ELEMENT UNDER THE INEXTENSIONAL CONSTRAINT

Figure 4 shows the nodal displacement vector of thin-walled curved beam elements considering the inextensibility condition (14). Because only the axial displacement term contains the third order derivative in the elastic strain energy (15), the axial displacement U_x and the remaining displacements U_y, θ are interpolated using Hermitian polynomials of the fifth and the third order respectively. As a results, this curved beam element has two nodes and seven nodal degrees of freedom and the element displacement functions can be assumed with respect to the nodal displacements as follows:

$$U_x = H_1 u^p + H_2\left(-\frac{w^p}{R}\right) + H_3\left(-\frac{\omega_2^p}{R}\right) + H_4 u^q + H_5\left(-\frac{w^q}{R}\right) + H_6\left(-\frac{\omega_2^q}{R}\right), \tag{54a}$$

$$U_y = h_1 v^p + h_2 \omega_3^p + h_3 v^q + h_4 \omega_3^q, \quad U_z = -R U_x', \tag{54b, c}$$

$$\theta = h_1 \omega_1^p - h_2 f^p + h_3 \omega_1^q - h_4 f^q, \tag{54d}$$

where

$$\begin{aligned} &u^p = U_x(0), \quad v^p = U_y(0), \quad w^p = R U_x'(0), \\ &\omega_1^p = \theta(0), \quad \omega_2^p = R U_x''(0), \quad \omega_3^p = U_y'(0), f^p = -\theta'(0) \end{aligned} \tag{55}$$

and H_i is the fifth order Hermitian polynomials as follows:

$$\begin{aligned} &H_1 = -6\xi^5 + 15\xi^4 - 10\xi^3 + 1, \quad H_2 = (-3\xi^5 + 8\xi^4 - 6\xi^3 + \xi)L, \\ &H_3 = (-0{\cdot}5\xi^5 + 1{\cdot}5\xi^4 - 1{\cdot}5\xi^3 + 0{\cdot}5\xi^2)L^2, \quad H_4 = 6\xi^5 - 15\xi^4 + 10\xi^3, \\ &H_5 = (-3\xi^5 + 7\xi^4 - 4\xi^3)L, \quad H_6 = (0{\cdot}5\xi^5 - \xi^4 + 0{\cdot}5\xi^3)L^2, \end{aligned} \tag{56}$$

Substituting equation (54) into equations (15) and (16) and integrating along the element length, the potential energy of the second curved beam element are the same as equation (43), but $\mathbf{K}_e$ and $\mathbf{M}_e$ become 14×14 element elastic stiffness and mass matrices respectively. In addition, a rotational nodal displacement including the curvature effect is defined as follows:

$$\widehat{\omega_2^p} = R U_x''(0) + \frac{U_x(0)}{R} = R\kappa_2^p + \frac{u^p}{R}. \tag{57}$$

Next, the transformation equation similar to equation (46) is obtained as follows:

$$\mathbf{U}_a = \mathbf{T}_2 \hat{\mathbf{U}}_a, \quad a = p, q. \tag{58}$$

where

$$\mathbf{U}_a^{\mathrm{T}} = \{u^a\ v^a\ w^a\ \omega_1^a\ \omega_2^a\ \omega_3^a\ f^a\}, \quad \widehat{\mathbf{U}_a^{\mathrm{T}}} = \{u^a\ v^a\ w^a\ \omega_1^a\ \widehat{\omega_2^a}\ \omega_3^a\ \widehat{f^a}\} \tag{59}$$

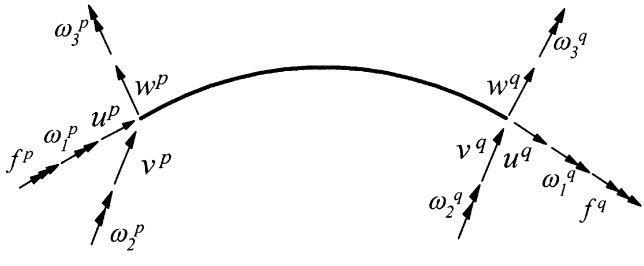

Figure 4. Nodal displacement vector of curved beam element with inextensional theory.

and

$$T_2 = \begin{bmatrix} 1 & \cdot & \cdot & \cdot & \cdot & \cdot & \cdot \\ \cdot & 1 & \cdot & \cdot & \cdot & \cdot & \cdot \\ \cdot & \cdot & -1/R & \cdot & \cdot & \cdot & \cdot \\ \cdot & \cdot & \cdot & 1 & \cdot & \cdot & \cdot \\ -1/R^2 & \cdot & \cdot & \cdot & 1/R & \cdot & \cdot \\ \cdot & \cdot & \cdot & \cdot & \cdot & 1 & \cdot \\ \cdot & \cdot & \cdot & \cdot & \cdot & 1/R & 1 \end{bmatrix}. \tag{60}$$

Through the similar procedure, the 14×14 element stiffness and mass matrices with respect to the element nodal displacement defined by equation (61) are evaluated and the eigenvalue problem corresponding to the thin-walled curved beam element under the inextensibility condition is constructed.

$$\hat{\mathbf{U}}_e = \langle u^p, v^p, w^p, \omega_1^p, \widehat{\omega_2^p}, \omega_3^p, \widehat{f^p}, u^q, v^q, w^q, \omega_1^q, \widehat{\omega_2^a}, \omega_3^a, \widehat{f^q} \rangle. \tag{61}$$

5. NUMERICAL EXAMPLES

The total potential energy functionals have been derived and analytical and numerical analysis procedures have been developed for spatial free vibrations of non-symmetric thin-walled curved beams. In this section, four numerical examples are presented to investigate the influence of thickness–curvature terms and inextensibility for decoupled and coupled vibration behaviors of curved beams according to the various values of subtended angle, length of beam and boundary conditions. Three types of analytical and numerical solutions (*CASE* 1, *CASE* 2, *CASE* 3) analysed by the present theory and method are presented and compared with previously published results or with solutions by ABAQUS' 9-noded shell element.

5.1. IN-PLANE FREE VIBRATION OF CURVED BEAMS WITH SQUARE CROSS-SECTIONS

In this example, for the purpose to compare the results by the proposed theory with those by Chidamparam and Leissa [8] based on the equation (22), in-plane vibration behaviors of the simply supported curved beam with square cross-sections are examined with keeping the radius constant but increasing the subtended angle. Material and geometrical data used for vibration analysis are follows:

$$E = 73\,000 \text{ kg/cm}^2, \quad \rho = 0{\cdot}00785 \text{ kg/cm}^3, \quad b = h = 1 \text{ cm}, R = 100 \text{ cm}.$$

The analytical solutions (*CASE* 1, *CASE* 2, *CASE* 2*, *CASE* 3) by this study for the lowest four frequencies of the hinged curved beam are presented in Table 1 with results by Chidamparam and Leissa's extensional and inextensional theory [8], in which *CASE* 2* denotes *CASE* 2 neglecting rotary inertia effects. Comparting the results by *CASE* 1 and *CASE* 3 under the extensional condition as well as those by *CASE* 2* and Chidamparam and Leissa [8] under inextensional condition, respectively, it can be noted that the curvature ratio h/R in this example is so small that the influence of thickness-curvature terms is negligible. However, it is found that for a small subtended angle there is a little differences due to rotary inertia between the results by *CASE* 3 Chidamparam and Leissa [8] under the extensional condition and those by *CASE* 2 and *CASE* 2* under the inextensional condition. The maximum difference due to rotary inertia effects is 4·1% and

TABLE 1

In-plane natural frequencies of simply supported beam ω^2

		Extensional theory			Inextensional theory		
Θ (deg)	Mode	Reference [8]	*CASE* 3	*CASE* 1	Reference [8]	*CASE* 2	*CASE* 2*
10	1	1564·99	1560·77	1556·79	12 965·5	12 827·7	12 965·7
	2	12 963·4	12 825·5	12 826·5	59 270·2	57 990·2	59 271·2
	3	65 897·8	64 336·4	64 335·5	208 049·0	199 445·0	208 053·0
	4	207 855·0	199 285·0	199 312·0	490 683·0	460 621·0	490 691·0
100	1	0·89978	0·89971	0·89976	0·89987	0·89981	0·89988
	2	5·20349	5·20249	5·20297	5·20804	5·20711	5·20811
	3	19·0183	19·0108	19·0120	19·0224	19·0152	19·0227
	4	46·7779	46·7489	46·7534	46·8831	46·8546	46·8839
180	1	0·03981	0·03981	0·03981	0·03982	0·03982	0·03982
	2	0·37139	0·37137	0·37139	0·37143	0·37142	0·37144
	3	1·51381	1·51366	1·51374	1·51399	1·51386	1·51401
	4	4·03414	4·03344	4·03369	4·03524	4·03460	4·03530
360	1	0·00000	0·00000	0·00000	0·00000	0·00000	0·00000
	2	0·00629	0·00629	0·00629	0·00629	0·00629	0·00629
	3	0·04638	0·04638	0·04638	0·04639	0·04639	0·04639
	4	0·16373	0·16372	0·16373	0·16374	0·16373	0·16374

6.1% at the fourth natural frequency for the subtended angle $\Theta = 10^\circ$ for the extensional and inextensional case respectively.

5.2. SIMPLY SUPPORTED CURVED BEAM WITH MONOSYMMETRIC SECTIONS

The simply supported beam and its monosymmetric cross-section are shown in Figure 5. Natural frequencies of thin-walled curved beams with the channel section monosymmetric for x_3 axis is investigated. Geometric and material properties of the monosymmetric cross-section defined at the centroidal axis are as follows:

$$A = 12{\cdot}5\,\text{cm}^2, \quad E = 73\,000\,\text{kg/cm}^2, \quad G = 28\,000\,\text{kg/cm}^2,$$
$$J = 1{\cdot}0417\,\text{cm}^4, \quad \rho = 0{\cdot}00785\,\text{kg/cm}^3, \quad I_2 = 133{\cdot}3854\,\text{cm}^4,$$
$$I_3 = 67{\cdot}9167\,\text{cm}^4, \quad I_{222} = -100{\cdot}0\,\text{cm}^5, \quad I_{233} = -41{\cdot}6667\,\text{cm}^5,$$
$$I_\phi = 5682{\cdot}1302\,\text{cm}^6, \quad I_{\phi 3} = -585{\cdot}1282\,\text{cm}^5, \quad I_{\phi 23} = -282{\cdot}0513\,\text{cm}^6,$$
$$I_{\phi\phi 2} = 7465{\cdot}7298\,\text{cm}^7, \quad L = 100\,\text{cm} \quad \text{and} \quad 400\,\text{cm}.$$

In this example, in-plane and out-of plane vibrational modes are decoupled and the curved beam is modelled by 20 curved beam elements. Also, the total beam length remains constant but the radius of curvature becomes small as the subtended angle is large. The natural frequencies corresponding to in-plane and out-of-plane modes are evaluated using both the analytical and numerical method developed in this study.

Tables 2 and 3 show the in-plane and out-of-plane natural frequencies for the various subtended angles of curved beams having the total length of 100 and 400 cm respectively. In the whole range of subtended angles, it is shown that the analytical solutions are in excellent agreement with results by the curved beam element. It is important to point out that the differences between results be *CASE* 1 including the thickness–curvature term and

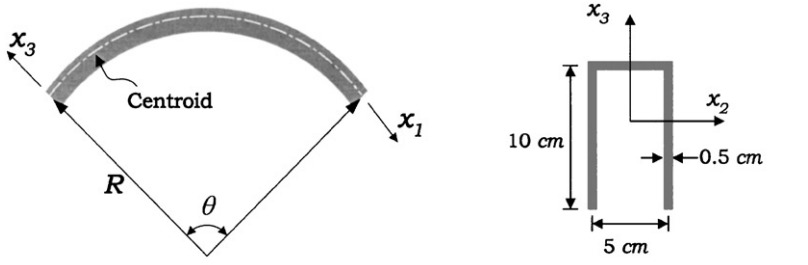

(a) Simply supported curved beam (b) Monosymmetric cross section

Figure 5. Shape of curved beam: (a) simply supported curved beam, (b) monosymmetric cross-section.

TABLE 2

In-plane natural frequencies of beam with monosymmetric section ω^2

			Analytical solution			Finite element method		
Length (cm)	Θ (deg)	Mode	*CASE* 1	*CASE* 2	*CASE* 3	*CASE* 1	*CASE* 2	*CASE* 3
		1	294·30	1442·2	297·96	294·30	1442·2	297·96
		2	1437·4	6452·5	1427·5	1437·4	6452·5	1427·5
	30	3	7131·4	21 126·0	7092·9	7131·9	21 126·0	7093·4
		4	9350·1	46576·0	9370·1	9350·1	46576·0	9370·1
		5	21 217·0	91 074·0	21 108·0	21 221·0	91 074·0	21 112·0
		1	1105·1	1127·0	1071·3	1105·1	1127·0	1071·3
		2	1800·3	5989·3	1810·2	1800·4	5989·3	1810·2
100	90	3	6890·8	20 218·0	6770·0	6891·3	20 218·0	6770·0
		4	10 586·0	45 950·0	10 691·0	10 586·0	45 950·0	10 691·0
		5	21 038·0	90 352·0	20 705·0	21 043·0	90 353·0	20 709·0
		1	490·17	501·74	460·54	490·18	501·74	460·55
		2	3884·9	4556·8	3577·8	3885·1	4556·8	3578·0
	180	3	9227·0	17 412·0	9343·1	9227·2	17 412·0	9343·4
		4	12 901·0	43 071·0	12 389·0	12 902·0	43 071·0	12 390·0
		5	21 574·0	86 912·0	21 841·0	21 577·0	86 912·0	21 844·0
		1	5·8260	5·8272	5·8194	5·8261	5·8272	5·8195
		2	12·256	27·107	12·257	12·256	27·107	12·258
	30	3	32·501	94·938	32·498	32·503	94·938	32·500
		4	94·879	223·60	94·768	94·899	223·60	94·788
		5	232·02	476·73	231·78	232·14	476·73	231·90
		1	4·4706	4·4759	4·4522	4·4707	4·4759	4·4523
		2	24·049	24·740	23·927	24·050	24·740	23·929
400	90	3	88·832	89·180	88·447	88·852	89·180	88·467
		4	126·16	216·91	126·17	126·17	216·91	126·18
		5	235·29	464·50	234·79	235·40	464·50	234·90
		1	1·9471	1·9498	1·9308	1·9471	1·9498	1·9308
		2	18·034	18·157	17·853	18·036	18·158	17·855
	180	3	73·209	73·687	72·469	73·228	73·687	72·488
		4	190·44	195·33	188·37	190·55	195·33	188·47
		5	420·78	428·76	416·24	421·25	428·76	416·71

TABLE 3

Out-of-plane natural frequencies of beam with monosymmetric section ω^2

			Analytical solution		Finite element method	
Length (cm)	Θ (deg)	Mode	*CASE* 1	*CASE* 3	*CASE* 1	*CASE* 3
		1	21·511	20·918	21·511	20·918
		2	99·481	101·34	99·481	104·34
	30	3	113·34	110·71	113·39	110·72
		4	466·64	455·94	466·66	455·97
		5	3269·0	3313·4	3269·1	3313·5
		1	5·0717	5·3208	5·0718	5·3210
		2	200·63	184·88	200·63	184·89
100	90	3	256·10	237·30	256·10	237·30
		4	608·92	566·87	608·96	566·90
		5	1685·4	1773·9	1685·4	1773·9
		1	0·0000	0·0000	0·0000	0·0000
		2	405·96	420·50	405·99	420·50
	180	3	550·83	501·14	550·86	501·19
		4	884·20	759·99	884·25	760·03
		5	1840·4	1678·6	1840·4	1678·6
		1	0·0694	0·0696	0·0694	0·0696
		2	2·0602	2·0496	2·0602	2·0496
	30	3	3·2747	3·2619	3·2747	3·2619
		4	4·4294	4·4044	4·4295	4·4045
		5	9·3022	9·3315	9·3025	9·3317
		1	0·0036	0·0036	0·0036	0·0036
		2	0·9167	0·9267	0·9168	0·9268
400	90	3	11·794	11·567	11·794	11·567
		4	18·709	18·395	18·709	18·395
		5	23·898	24·206	23·904	24·212
		1	0·0000	0·0000	0·0000	0·0000
		2	0·0971	0·0981	0·0972	0·0982
	180	3	3·9362	4·0409	3·9394	4·0442
		4	60·272	57·932	60·274	57·935
		5	113·76	111·22	113·76	111·22

those by *CASE* 3 neglecting it increase as the subtended angle becomes large. Furthermore, for the identical subtended angle, the influence of thickness–curvature terms is decreased as the slenderness is large. Particularly, it should be noted that the in-plane vibration analysis under the inextensibility condition (*CASE* 2) leads to the erroneous results as the slenderness is small. As a result, it is judged that the present curved beam theory considering the thickness–curvature effect and allowing the extensibility gives accurate results for the out-of-plane as well as in-plane vibrations of the monosymmetric curved beams.

5.3. CLAMPED SEMICIRCULAR BEAMS WITH Z-SECTIONS

In this example, for the freely vibrating clamed semicircular beam with Z-sections of equal and unequal flanges as shown in Figure 6, numerical solutions by the proposed

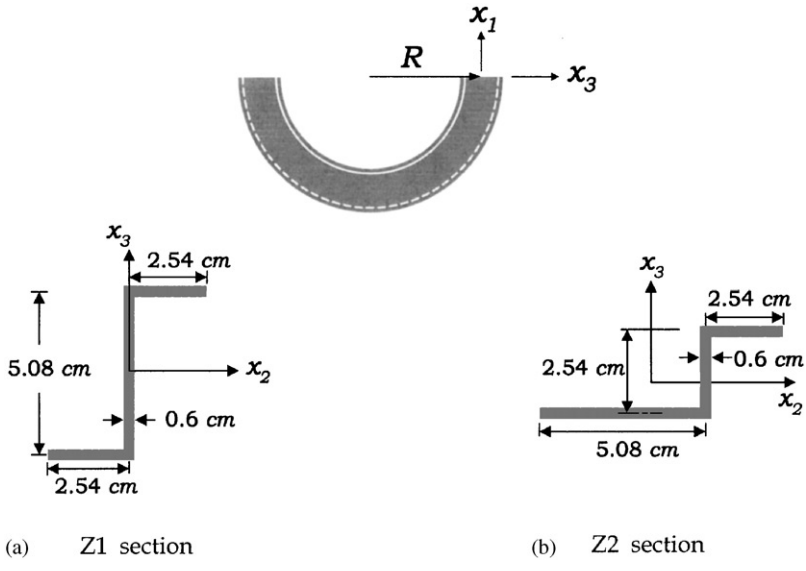

(a) Z1 section (b) Z2 section

Figure 6. Thin-walled semicircular beams with Z-cross-sections: (a) Z1 section, (b) Z2 section; $E = 730\,887\,\text{kg/cm}^2$, $R = 100{\cdot}0\,\text{cm}$, $\rho = 0{\cdot}002768\,\text{kg/cm}^3$.

TABLE 4

Natural frequencies of clamped semicircular beam ω^2

	Z1 section					Z2 section				
	This study			Reference	Shell	This study			Reference	Shell
Mode	*CASE* 1	*CASE* 2	*CASE* 3	[30]	[36]	*CASE* 1	*CASE* 2	*CASE* 3	[30]	[36]
1	4·8963	4·8986	4·9086	4·8993	4·5199	6·3765	6·3718	6·3873	6·0800	6·0800
2	23·252	23·252	23·360	23·852	22·777	21·520	21·521	21·495	21·497	21·103
3	107·90	107·90	108·69	114·06	105·60	74·416	74·380	74·640	71·107	76·917
4	166·50	166·79	166·86	168·55	156·79	104·68	104·76	104·56	120·77	102·28
5	336·97	336·97	339·89	335·82	329·87	340·75	341·00	340·95	332·91	339·32

methods are compared with the results by Gendy and Saleeb [30] and those by the shell element model taken from reference [36].

Table 4 shows the lowest five vibration frequencies for the two types of cross-sections. In Table 4, it is observed that the results by the present three models (*CASE* 1, *CASE* 2, *CASE* 3) are nearly identical to each other and is slightly better that those by Gendy and Saleeb' model [30] when comparing with those using the shell element. Because the slenderness is relatively large in this example, it turns that the thickness–curvature and the inextensibility have little effects on the free vibration of the clamped curved beam.

5.4. CANTILEVER AND CLAMPED CURVED BEAMS WITH NON-SYMMETRIC SECTIONS

The spatial free vibration analysis of non-symmetric curved beams is performed for the various subtended angles with clamped–free and clamped–clamped boundary conditions

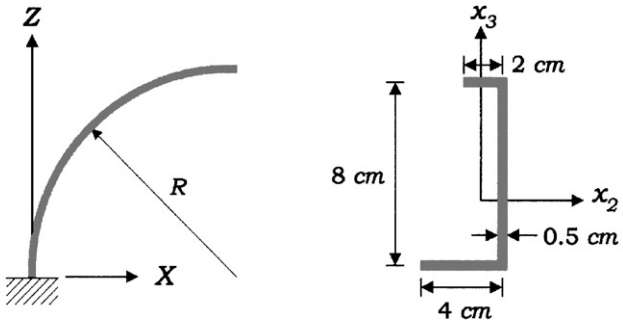

Figure 7. Thin-walled cantilever beam with non-symmetric cross-section: (a) Geometry of curved beam, (b) cross-section.

at both ends. Figure 7 shows a thin-walled curved cantilever beam with non-symmetric cross-section. The curved beam is modelled using 20 curved beam elements and 300 shell elements of ABAQUS which is the commercial finite element analysis program respectively. Geometric and material properties for analysis are given as follows:

$$A = 7{\cdot}0\,\text{cm}^2, \quad E = 30\,000\,\text{kg/cm}^2, \quad G = 11\,500\,\text{kg/cm}^2,$$
$$J = 0{\cdot}5833\,\text{cm}^4, \quad \rho = 0{\cdot}00785\,\text{kg/cm}^3, \quad I_2 = 67{\cdot}0476\,\text{cm}^4,$$
$$I_3 = 8{\cdot}4286\,\text{cm}^4, \quad I_{23} = 9{\cdot}1429\,\text{cm}^4, \quad I_{222} = 52{\cdot}2449\,\text{cm}^5,$$
$$I_{233} = -20{\cdot}0272\,\text{cm}^5, \quad I_{223} = -17{\cdot}4150\,\text{cm}^5, \quad I_{333} = -13{\cdot}3878\,\text{cm}^5,$$
$$I_\phi = 272{\cdot}5442\,\text{cm}^6, \quad I_{\phi 2} = 115{\cdot}8095\,\text{cm}^5, \quad I_{\phi 3} = 30{\cdot}4762\,\text{cm}^5,$$
$$I_{\phi 22} = 59{\cdot}2109\,\text{cm}^6, \quad I_{\phi 23} = -107{\cdot}1020\,\text{cm}^6, \quad I_{\phi 33} = -63{\cdot}1293\,\text{cm}^6,$$
$$I_{\phi\phi 2} = 67{\cdot}1720\,\text{cm}^7, \quad I_{\phi\phi 3} = -388{\cdot}7269\,\text{cm}^7, \quad L = 200\,\text{cm}.$$

Table 5 shows the lowest 10 frequencies of curved cantilever for subtended angles varying from 10° to 180° with keeping the total length of the cantilever constant. It is found from Table 5 that the results by *CASE* 1 are in a good agreement with those by ABAQUS's shell elements. Particularly, the influence of thickness–curvature increases up to the maximum difference 43·1% at the ninth mode for the subtended angle $\Theta = 180°$ as the subtended angle becomes large, but the effect of inextensibility is negligible irrespective of the variation of subtended angle.

On the other hand, Table 6 shows the lowest 10 frequencies of the curved beam clamped at both ends with the varying subtended angles. It is interesting to observe that for clamped curved beam, the thickness–curvature effect is relatively small (the maximum difference 8·2% at the tenth mode for $\Theta = 180°$) when comparing with cantilever curved beam, but the differences between results by *CASE* 1 and those by *CASE* 2 corresponding to the extensional and inextensional condition, respectively, are noticeable for the small subtended angles and subsequently decrease as the angle becomes large.

TABLE 5

Natural frequencies of non-symmetric cantilever curved beam ω^2

		Vibration mode									
Θ (deg)	*CASE*	1	2	3	4	5	6	7	8	9	10
10	1	0·0290	0·2686	0·5963	1·5252	5·1373	7·7438	17·386	20·623	27·159	52·344
	2	0·0290	0·2686	0·5963	1·5252	5·1376	7·7440	17·387	20·625	27·161	52·346
	3	0·0290	0·2726	0·6417	1·6072	5·1856	7·7975	17·396	20·679	27·288	52·499
	ABAQUS	0·0299	0·2670	0·5887	1·5265	5·0520	7·7433	16·925	20·575	26·645	52·892
30	1	0·0212	0·2815	0·3747	2·2666	5·0554	7·4328	19·493	20·511	28·177	49·067
	2	0·0212	0·2815	0·3747	2·2666	5·0576	7·4356	19·499	20·520	28·206	49·081
	3	0·0225	0·2825	0·5146	3·2566	5·0755	8·3196	19·695	20·662	29·243	49·820
	ABAQUS	0·0213	0·2791	0·3724	2·2487	5·0275	7·3378	19·518	19·935	27·449	49·227
60	1	0·0107	0·2480	0·3084	2·3788	5·8332	7·1242	18·221	28·219	31·332	44·828
	2	0·0107	0·2480	0·3084	2·3788	5·8502	7·1246	18·228	28·222	31·439	44·879
	3	0·0128	0·2666	0·4267	3·6090	5·8462	11·810	21·142	28·050	33·768	49·133
90	1	0·0062	0·2061	0·2901	2·0272	5·2139	7·3646	17·473	32·844	37·949	47·721
	2	0·0062	0·2061	0·2901	2·0272	5·2345	7·3687	17·476	33·022	37·951	47·823
	3	0·0072	0·2554	0·3499	3·0204	5·3567	11·999	29·567	32·644	40·216	59·173
	ABAQUS	0·0060	0·2043	0·2779	2·1714	5·0293	7·1815	17·079	32·233	36·624	43·574
120	1	0·0043	0·1608	0·2945	1·6893	4·3515	7·0502	16·728	34·383	36·373	67·954
	2	0·0043	0·1608	0·2946	1·6894	4·3670	7·0564	16·729	34·654	36·404	67·994
	3	0·0047	0·2223	0·3154	2·5051	4·5662	10·733	29·483	34·388	57·156	69·610
150	1	0·0034	0·1222	0·3141	1·3938	3·6529	6·4512	15·798	33·813	34·377	68·559
	2	0·0034	0·1222	0·3143	1·3939	3·6627	6·4564	15·797	34·068	34·466	68·569
	3	0·0042	0·1693	0·3279	2·0697	3·8755	9·4714	26·832	34·092	61·301	90·192
180	1	0·0030	0·0929	0·3462	1·1389	3·1403	5·7825	14·724	31·503	32·765	64·026
	2	0·0030	0·0929	0·3464	1·1389	3·1459	5·7861	14·724	31·742	32·852	64·045
	3	0·0047	0·1248	0·3607	1·6979	3·3532	8·3370	24·186	32·119	57·632	108·30

6. CONCLUSIONS

Three types of the total potential energy depending on whether the thickness–curvature effect and the extensional condition are taken into account or not were presented by applying the principle of virtual work and considering the restrained warping effects based on Vlasov's assumption. Not only analytical solutions were exactly derived for in-plane and out-of-plane free vibration of monosymmetric thin-walled curved beam, but also numerical solutions by the two curved beam elements and ABAQUS' shell elements were presented for spatial free vibration analysis. Through numerical examples, effects of thickness–curvature and the extensibility condition were investigated on the spatial vibrational behavior according to the various values of subtended angle, length of beam and boundary conditions. Consequently it is judged that the analytical and numerical method by the curved beam theory (*CASE* 1) considering the thickness–curvature effects as well as the extensional condition provides accurate solutions for spatial free vibration problems of non-symmetric thin-walled curved beams though the slenderness or the radius of curvature are relatively small.

TABLE 6

Natural frequencies of non-symmetric clamped curved beam ω^2

		Vibration mode									
Θ (deg)	*CASE*	1	2	3	4	5	6	7	8	9	10
10	1	0·9488	4·4120	6·3262	17·732	18·778	21·295	49·634	59·534	99·775	119·58
	2	0·9493	6·3262	9·2795	18·779	20·772	49·633	56·592	99·571	119·60	147·68
	3	0·9499	4·4051	6·3430	17·747	18·732	21·362	49·847	59·341	100·24	119·61
	ABAQUS	0·9679	4·3543	6·4045	16·946	18·565	21·369	50·231	58·585	100·44	105·01
30	1	0·8338	5·3737	10·799	18·125	22·087	31·469	45·206	68·388	93·079	123·91
	2	0·8338	5·3737	13·512	18·437	22·090	45·206	62·435	92·940	124·05	158·82
	3	0·8359	5·4161	10·723	18·322	21·931	31·500	45·787	67·772	94·364	123·88
	ABAQUS	0·8479	5·4097	10·605	18·235	21·878	30·386	45·524	67·401	93·276	107·62
60	1	0·7753	4·4992	15·392	24·041	27·515	39·667	60·538	84·626	104·35	131·16
	2	0·7762	4·4992	15·398	25·143	27·539	39·667	71·000	84·752	131·60	155·73
	3	0·7759	4·5586	15·721	23·694	27·207	40·663	60·169	86·752	103·51	130·79
90	1	0·7223	3·9916	13·570	31·829	35·223	41·852	71·047	80·658	138·20	148·88
	2	0·7235	3·9916	13·584	31·917	35·222	42·313	73·552	83·604	138·38	149·59
	3	0·7216	4·0530	13·962	31·475	36·513	41·029	71·677	81·803	139·78	151·96
	ABAQUS	0·7020	3·9088	13·388	30·838	34·855	37·792	69·831	78·659	115·15	140·53
120	1	0·6446	3·6238	12·257	31·523	33·616	64·519	68·869	86·169	130·81	165·18
	2	0·6454	3·6238	12·270	31·534	33·792	64·526	69·404	90·072	130·81	166·21
	3	0·6443	3·6829	12·670	32·459	33·912	63·567	71·618	84·685	138·23	162·03
150	1	0·5522	3·2906	11·259	28·378	32·733	62·680	90·153	96·772	121·55	193·33
	2	0·5527	3·2906	11·269	28·400	32·980	62·806	91·901	98·694	121·57	194·13
	3	0·5538	3·3493	11·673	29·560	33·070	66·801	88·379	93·820	130·46	187·23
180	1	0·4589	2·9571	10·422	25·347	30·400	58·225	93·334	113·14	131·99	200·85
	2	0·4592	2·9570	10·429	25·400	30·642	58·290	96·387	113·17	132·22	201·02
	3	0·4626	3·0185	10·830	26·378	31·101	62·694	91·594	122·99	127·40	218·69

ACKNOWLEDGMENTS

The authors are grateful for the support provided by a grant from the Korea Research Foundation (K.R.F.) and Safety and Structural Integrity Research Center at the Sungkyun kwan University.

REFERENCES

1. P. RAVEENDRANATH, G. SINGH and B. PRADHA 2000 *Computers & Structures* **78**, 583–590. Free vibration of arches using a curved beam element based on a coupled polynomial displacement field.
2. S. J. OH, B. K. LEE and I. W. LEE 1999 *Journal of Sound and Vibration* **219**, 23–33. Natural frequencies of non-circular arches with rotatory inertia and shear deformation.
3. T. TARNOPOLSKAYA and F. R. DE HOOG 1999 *Journal of Sound and Vibration* **228**, 69–90. Low-frequency mode transition in the free in-plane vibration of curved beams.
4. T. TARNOPOLSKAYA, F. R. DE HOOG, N. H. FLETCHER and S. THWAITES 1996 *Journal of Sound and Vibration* **196**, 659–680. Asymptotic analysis of the free in-plane vibrations of beams with arbitrarily varying curvature and cross-section.

5. A. Krishnan, and Y. J. Suresh 1998 *Computers & Structures* **68**, 473–489. A simple cubic linear element for static and free vibration analysis of curved beams.
6. C. S. Huang, Y. P. Tseng, A. W. Leissa and K. Y. Nieh 1998 *International Journal of Mechanical Sciences* **40**, 1159–1173. An exact solution for in-plane vibrations of an arch having variable curvature and cross section.
7. Y. P. Tseng, C. S. Huang and C. J. Lin 1997 *Journal of Sound and Vibration* **207**, 15–31. Dynamic stiffness analysis for in-plane vibrations of arches with variable curvature.
8. P. Chidamparam and A. W. Leissa 1995 *Journal of Sound and Vibration* **183**, 779–795. Influence of centerline extensibility on the in-plane free vibrations of loaded circular arches.
9. J. P. Charpie and C. B. Burroughs 1993 *Journal of the Acoustical Society of America* **94**, 866–879. An analytic model for the free in-plane vibration of beams of variable curvature and depth.
10. J. F. M. Scott and J. Woodhouse 1992 *Philosophical Transactions of the Royal Society of London, Physical Sciences and Engineering* **339**, 587–625. Vibration of an elastic strip with varying curvature.
11. K. Suzuki and S. Takahashi 1982 *Bulletin of the Japan Society of Mechanical Engineers* **25**, 1100–1107. In-plane vibration of curved bars with varying cross-section.
12. T. Irie, G. Yamada and I. Takahashi 1980 *Bulletin of the Japan Society of Mechanical Engineers* **23**, 567–573. In-plane vibration of a free–clamped slender arc of varying cross-section.
13. M. Petyt and C. C. Fleischer 1971 *Journal of Sound and Vibration* **18**, 17–30. Free vibration of a curved beam.
14. A. K. Gupta and W. P. Howson 1994 *Journal of Sound and Vibration* **175**, 145–157. Exact natural frequencies of plane structures composed of slender elastic curved members.
15. B. K. Lee and J. F. Wilson 1989 *Journal of Sound and Vibration* **136**, 75–89. Free vibrations of arches with variable curvature.
16. M. S. Issa, T. M. Wang and B. T. Hsiao 1987 *Journal of Sound and Vibration* **114**, 297–308. Extensional vibrations of continuous circular curved beams with rotary inertia and shear deformation, I: free vibration.
17. T. M. Wang and M.P. Guilbert 1981 *International Journal of Solids and Structures* **17**, 281–289. Effects of rotary inertia and shear on natural frequencies of continuous circular curved beams.
18. T. M. Wang 1972 *Journal of Structural Division* **98**, 407–411. Lowest natural frequency of clamped parabolic arcs.
19. A.S. Veletos, W.J. Austin, C.A. Lopes and S.J. Wung 1972 *Journal of Engineering Mechanics Division* **98**, 311–329. Free in-plane vibration of circular arches.
20. M. T. Piovan, V. H. Cortinez and R. E. Rossi 2000 *Journal of Sound and Vibration* **237**, 101–118. Out-of-plane vibrations of shear deformable continuous horizontally curved thin-walled beams.
21. W. P. Howson and A. K. Jemah 1999 *Journal of Engineering Mechanics* **125**, 19–25. Exact out-of-plane natural frequencies of curved Timoshenko beams.
22. W. P. Howson and A. K. Jemah and J. Q. Zhou 1995 *Computers & Structures* **55**, 989–995. Exact natural frequencies for out-of-plane motion of plane structures composed of curved beam members.
23. J. M. Snyder and J. F. Wilson 1992 *Journal of Sound Vibration* **157**, 345–355. Free vibrations of continuous horizontally curved beams.
24. T. M. Wang and W. F. Brannen 1982 *Journal of Sound and Vibration* **84**, 241–246. Natural frequencies for out-of-plane vibrations of curved beams on elastic foundations.
25. T. M. Wang, R. H. Nettleton and B. Keita 1980 *Journal of Sound and Vibration* **68**, 427–436. Natural frequencies for out-of-plane vibrations of continuous curved beams.
26. K. Suzuki, H. Aida and S. Takahashi 1978 *Bulletin of the Japan Society of Mechanical Engineers* **21**, 162–173. Vibrations curved bars perpendicular to their planes.
27. S. Takahashi and K. Suzuki 1977 *Bulletin of the Japan Society of Mechanical Engineers* **20**, 1409–1416. Vibrations of elliptic arc bar perpendicular to their planes.
28. M. Kawakami, T. Sakiyama, H. Matsuda and C. Morita 1995 *Journal of Sound and Vibration* **187**, 381–401. In-plane and out-of-plane free vibrations of curved beams with variable sections.
29. K. Kang, C. W. Bert, and A. G. Striz 1995 *Journal of Sound and Vibration* **181**, 353–360. Vibraion analysis of shear deformable circular arches by the differential quadrature method.
30. A. S. Gendy and A. F. Saleeb 1994 *Journal of Sound and Vibration* **174**, 261–274. Vibration analysis of coupled extensional/flexural/torsional modes or curved beams with arbitrary thin-walled sections.

31. M. Y. Kim, B. C. Min and M. W. Shu 2000 *Journal of Engineering Mechanics* **126**, 497–505. Spatial stability of nonsymmetric thin-walled curved beams. I: analytic approach.
32. M. Y. Kim, B. C. Min and M. W. Shu 2000 *Journal of Engineering Mechanics* **126**, 506–514. Spatial stability of nonsymmetric thin-walled curved beams. II: numerical approach.
33. ABAQUS 1992 *User's Manual Vols. I and II*, Ver. 5.2. Hibbit, Karlsson & Sorensen, Inc.
34. A. E. H. Love 1934 *A Treatise on the Mathematical Theory of Elasticity*. Cambridge: Cambridge University Press; fourth edition.
35. S. B. Kim and M. Y. Kim 2000 *Engineering Structures* **25**, 446–458. Improved formulation for spacial stability and free vibration of thin-walled tapered beam and space frames.
36. A. K. Noor, J. M. Peters and B. J. Min 1989 *Finite Elements in Analysis and Design* **5**, 291–305. Mixed finite element models for free vibrations of thin-walled beams.